Research Article | Vol. 29, No. 21 / 11 Oct 2021 / Optics Express 34590
Optics EXPRESS

Quantum limited timing jitter of soliton molecules in a mode-locked fiber laser

DEFENG ZOU,[1] ZEQING LI,[1] PENG QIN,[2,3] YOUJIAN SONG,[1,4] AND MINGLIE HU[1]

[1] *Ultrafast Laser Laboratory, Key Laboratory of Opto-Electronic Information Science and Technology of Ministry of Education, School of Precision Instruments and Opto-electronics Engineering, Tianjin University, Tianjin 300072, China*
[2] *Qian Xuesen Laboratory of Space Technology, China Academy of Space Technology, Beijing 100094, China*
[3] *qinpeng@qxslab.cn*
[4] *yjsong@tju.edu.cn*

Abstract: Soliton molecules in mode-locked lasers are expected to be ideal self-organization patterns, which warrant stability and robustness against perturbations. However, recent ultra-high resolution optical cross-correlation measurements uncover an intra-molecular timing jitter, even in stationary soliton molecules. In this work, we found that the intra-molecular timing jitter has a quantum origin. Numerical simulation indicates that amplified spontaneous emission (ASE) noise induces a random quantum diffusion for soliton pulse timing, which cannot be compensated by soliton binding mechanism. By suppressing indirectly coupled timing jitter at close-to-zero cavity dispersion, a record-low 350 as rms intra-soliton-molecular jittering is obtained from an Er-fiber laser in experiment. This work provides insight into the fundamental limits for the instability of multi-soliton patterns.

1. Introduction

Passively mode-locked lasers, known as complex nonlinear systems, have substantial intracavity pulse dynamics. The balance among nonlinearity, dispersion as well as dissipation regularly allows dissipative soliton formation. In particular, soliton interactions produce various bound states, which are often known as soliton molecules in analogy with matter molecules formed by chemical bonds. Recently, soliton molecules have attracted extensive attention due to their fundamental significance on the study of attractive and repulsive behaviors of solitons in nonlinear dissipative systems [1]. Moreover, soliton molecules hold potential to provide a multilevel encoding pattern in optical telecommunication systems [2]. The first theoretical prediction of soliton molecules was provided by Malomed [3]. Subsequently, a great variety of investigations have revealed profound soliton-molecular dynamics, basically, relying on averaging measurement conducted by optical spectrum analyzers and auto-correlators [4–7]. Further in-depth investigations require advanced probing methods. Time-stretched dispersive Fourier-transform (TS-DFT) technique [8], which is capable of mapping real time optical spectrum into time-stretched waveform by a segment of large dispersive material, provides an ideal tool to the study of transient optical phenomena [9–13]. TS-DFT technique has been successfully applied to resolve soliton molecular dynamics, in terms of real-time evolution of the pulse separation ρ and phase difference φ between the pulses [14–23]. However, the temporal resolution for resolving the evolution of binding separation is limited to picoseconds. Recently, we showed that optical cross-correlation (OC) technique can significantly improve the temporal resolution to sub-femtosecond level in fiber lasers and attoseconds level in a Kerr-lens mode-locked Ti: sapphire laser. Power spectral analysis of the intriguing soliton molecular dynamics is also allowed [24,25].

#437553 https://doi.org/10.1364/OE.437553
Journal © 2021 Received 12 Jul 2021; revised 24 Sep 2021; accepted 29 Sep 2021; published 8 Oct 2021

Optics EXPRESS

The random walk of optical solitons originated from the ASE noise and thus quantum-limited timing jitter determines its fundamental limits in applications of time-of-flight distance measurements, optical communication systems, optical frequency comb, to name only a few [26]. From the theoretical perspective, the study of quantum-limited fluctuations between optical solitons is essential to uncover intrinsic soliton interaction mechanisms. For this purpose, a few groups have investigated the relative timing jitter between optical solitons circulating in one optical cavity, where the technical noises are common-mode noises and are cancelled out by sharing the cavity. Our group firstly revealed the quantum-limited relative timing jitter between optical solitons in a dual-wavelength mode-locked Er-fiber laser, which simultaneously generates a pair of solitons with an offset repetition rate in a shared cavity [27]. Recent experiments also verified a quantum diffusion between two Kerr-solitons from a bidirectional silica wedge micro-resonator [28]. Even though random fluctuations within robust soliton patterns have also been characterized recently [24,25,29], the physical origin has not been well interpreted.

In this paper, we investigate the relative timing jitter of intra-soliton-molecular pulses separation within soliton molecules in a fiber laser. Numerical simulation suggests that the solitons are bounded with a limited bandwidth in the presence of ASE noise. The cutoff frequency is related closely to the binding strength and ASE noise. The quantum limited timing jitter increase with soliton separation. We further experimentally characterize the intra-molecular timing jitter by optical cross-correlation (OC) method. By optimizing the net cavity dispersion (NCD) which significantly reduces Gordon-Haus jitter [30], overall timing jitter as low as 350 as is achieved for 0.49 ps soliton separation. By excluding the noise contributions of the technical noise, the intra-molecular quantum limited timing jitter is well below 300 as. These results shed light on further understanding of close-range soliton interaction dynamics and pave the way for future applications in complex nonlinear systems.

2. Numerical simulation and results

In the aspect of numerical simulation, nonlinear Schrödinger equation (NLSE) holds the ability to reproduce stable mode-locked state and complex sequential instabilities in fiber lasers [31]. Internal motion dynamics of soliton molecules, such as oscillating phase, diverging sliding phase as well as variable intra-soliton-molecular separation have been investigated [32]. However, numerical results refer to quantum limited timing jitter of soliton molecular binding separation have not been reported yet.

We consider a dispersion-managed mode-locked Er-doped fiber laser, as shown in Fig. 1(a). The pulse dynamics is reconstructed by the well-established split-step Fourier transform method. The simulated model contains a segment of Er-doped fiber (EDF), two segments of single mode fiber (SMF1 and SMF2), an output coupler (OC) and a saturable absorber (SA). The pulse propagation in optical fiber is modeled by the modified NLSE [33]:

$$\frac{\partial A}{\partial z} + \frac{i}{2}\left(\beta_2 + ig\frac{1}{\Omega_g{}^2}\right)\frac{\partial^2 A}{\partial \tau^2} = \frac{g}{2}A + \frac{\beta_3}{6}\frac{\partial^3 A}{\partial \tau^3} + i\gamma|A|^2 A + S_{pert} \tag{1}$$

where $A = A\ (z, \tau)$ is the field envelope with z the propagation coordinate and τ the time-delay parameter. β_2, β_3 and γ are the second order dispersion, third order dispersion and nonlinear coefficients, respectively. $g = g_0/(1+\int|A|^2 d\tau/E_{sat}+(\omega-\omega_0)/\Delta\omega^2)$ is the EDF gain, where g_0 is the small-signal gain, E_{sat} is the saturation energy, ω is the optical angular frequency, ω_0 is the central angular frequency, $\Delta\omega$ is gain bandwidth. S_{pert} is the ASE noise source term added as white noise across the optical spectrum. According to the semi-classical noise theory, amplitude of the ASE accumulated within a unit bandwidth after a propagation step h inside the gaining fiber is $\Delta A_{ASE} = \theta\hbar(\exp(gh)\text{-}1$ [34]. By taking into account the parabolic gaining spectrum, the

Optics EXPRESS

spectral characteristics of the Fourier transform of S_{pert} is given by [35,36]:

$$\left\langle \tilde{S}(z,\omega)\tilde{S}(z',\omega')\right\rangle = \frac{1}{2\pi}\frac{1}{((\omega-\omega_0)/\Delta\omega)^2+1}\frac{\theta\hbar\omega(\exp(gh)-1)}{h}\delta(z-z')\delta(\omega-\omega') \quad (2)$$

where $S(z,\omega)$ is the Fourier transform of $S(z,\tau)$ and Angle brackets represents the correlation function. δ represents Dirac's delta functions and here simply indicates that components at different frequencies are uncorrelated. $\hbar$ is the Planck constant, and h is the gain fiber length. $\theta = 10$ is the enhanced spontaneous emission factor due to incomplete inversion of the gain medium [37]. We use the Eq. (2) for frequency domain integration, and the obtained integral value is used as amplitude of Gaussian white noise generated by computer. The SA is modeled by a power dependent transmittance function:

$$T(\tau) = 1 - \alpha_{ns} - q_0(1 + P/P_{sat})^{-1} \quad (3)$$

where q_0 is modulation depth, α_{ns} is the non-saturable loss, $P = |A|^2$ is instantaneous power, P_{sat} is saturation power. Parameters of the simulation are as follows: Length of the gain fiber is 0.9 m. The gain bandwidth of the EDF is set as 50 nm and centered at 1550 nm. The small-signal gaining coefficient is 1.38/m and the output coupling rate is 20%. The SA is modeled with 8% non-saturable loss, 30% modulation depth and 50 W saturation power. The group velocity dispersion (GVD) of EDF and SMF are 0.03277 ps^2/m and -0.022 ps^2/m, respectively. Length of SMF 1 is 1 m, while that of SMF 2 is adjusted from 1 m to 0.4 m. The optimized NCD used for the soliton molecules with narrowest pulses separation is -0.002 ps^2.

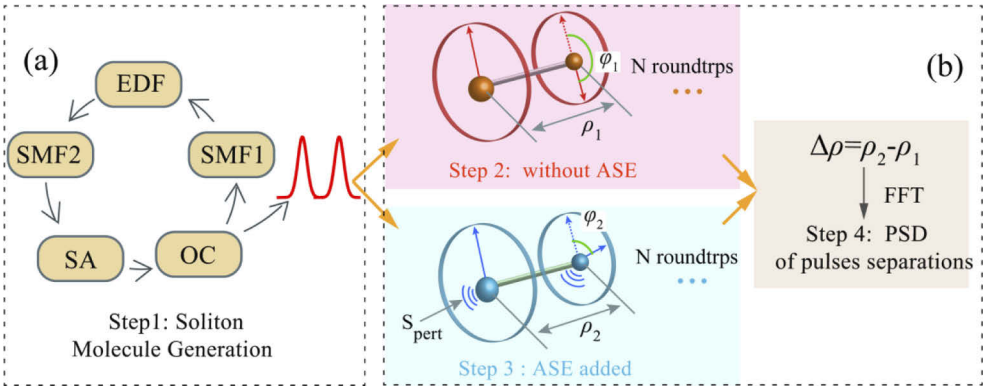

Fig. 1. (a) Step 1: illustration of the fiber laser cavity elements used for the simulations and soliton molecules generation. EDF: Er-doped fiber; SMF: single-mode fiber; SA: saturable absorber, OC: output coupler. (b) Illustration of quantum diffusion of intra-soliton-molecular pulses in the simulation. Step 2: soliton molecules without ASE. Step 3: soliton molecules with ASE. ρ represents the intra-molecular temporal separation and the angle φ corresponds to the relative phase in Step 4.

In order to obtain the intra-molecular quantum limited timing jitter of pulse separation introduced by ASE, two independent cavity models are conducted after converged states have been obtained, as shown in Fig. 1(b). In the simulation, the converged states are assumed to be the case that the relative change of soliton-molecular energy is lower than 10^{-8} between two consecutive round trips. Once the intra-cavity soliton molecules are converged, they are used as incident pulses for both models. Firstly, a sequence of temporal pulse separations of the soliton molecule in the absence of ASE noise are calculated, serving as the reference ρ_1. Then, we repeat the same operation with ASE noise added into the EDF during every roundtrip. A

Optics EXPRESS

sequence of temporal pulse separations ρ_2 are used as targets. The timing jitter PSD spectra is Fourier-transformed from the temporal deviation $\Delta\rho$ between ρ_2 and ρ_1. By integrating PSD, the rms quantum limited timing jitter of pulse separations can be obtained [35,36].

Stable mode-locked state can be built up from noise after several dozens of roundtrips. As shown in Fig. 2(a), two intra-molecular pulses evolve from the noise background directly and stabilize gradually. The single pulse width is 260 fs. Figure 2(b) plots the corresponding spectral evolution. The high contrast spectral interference fringes and high stability of optical spectrum are typical characteristics of stationary soliton molecules. Then, the stable soliton molecule is used as the incident pulse to propagate in the cavity without ASE noise. As shown in Fig. 2(c), the intra-molecular temporal separation is 13.047 ps, which matches with the modulation period of the optical spectral fringe of 6.2 nm. The variation of pulses separation less than 0.001 ps during 5000 cavity roundtrips, linked to strong binding strength between leading and trailing pulses in the soliton molecule and the great ability to resist external disturbance. The relative phase between two pulses slides from 0.22 to 0.32 rad, resulting in the slight deviation from fixed point on the interaction planes shown in Fig. 2(d) [20].

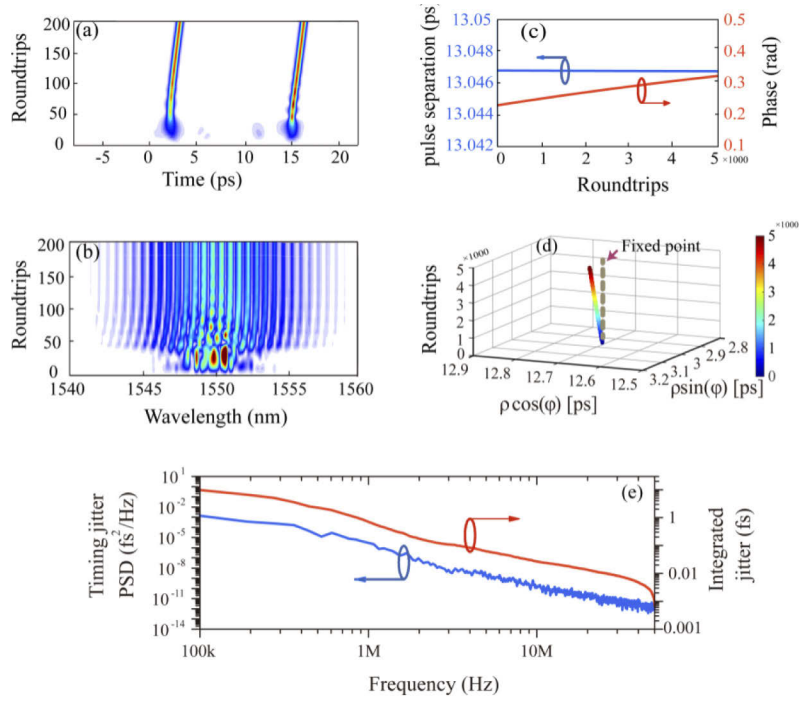

Fig. 2. Numerical simulations of intra-soliton-molecular motion (a) time domain and (b) spectral evolution from stochastic white noise; (c) soliton molecular pulse separation, relative phase and (d) interaction planes, as a function of cavity round trips. (e) Timing jitter PSD and corresponding integrated quantum limited timing jitter of pulses separation.

In the following, the stable soliton molecule is used as the incident pulse to propagate in the cavity with ASE noise, to obtain the ASE-induced quantum limited timing jitter. As presented in Fig. 2(e), the timing jitter PSD of pulse separation (blue curve) rolls off at a -20 dB/decade slope throughout the whole frequency range (from 100 kHz to Nyquist frequency of ~50 MHz). The corresponding integrated quantum limited timing jitter is 7.3 fs, as indicated by red curve.

Besides intra-soliton-molecular pulse separation of 13.05 ps, soliton molecules with pulse separation of 0.86 ps, 0.98 ps, and 6.15 ps are also obtained. The timing jitter PSD curves at the

Optics EXPRESS

above three pulse separations are presented in Fig. 3. The rms quantum limited timing jitters integrated from 100 kHz to 40 MHz are expressed in the inset of Fig. 3. The timing jitter PSD shows lowpass characteristic with an obvious cutoff frequency. Take the PSD curve of 0.86 ps as an example, the timing jitter PSD characteristics -20 dB/decade slope beyond the cutoff frequency of ~ 3 MHz. This suggests that the quantum diffusion within soliton molecules dominates the intra-soliton-molecular motion over a short timescale < 0.33 μs. On a timescale exceeding 0.33 μs (frequency range < 3 MHz), quantum-limited soliton diffusion within soliton molecules is constrained, which is attributed to the binding force of leading and trailing pulses. For soliton molecules with larger pulse separation, the cutoff frequency shifts to lower frequency range, which is ~ 2 MHz and 5 kHz for the case of 0.98 ps and 6.15 ps pulse separation, respectively. The reduced cutoff frequency with larger pulses separation indicates a weakened binding strength and thus increased quantum-limited timing jitter. Overall, the simulation results show that pulses within soliton molecules are bounded with limited bandwidth. The quantum-limited diffusion within soliton molecules plays a leading role beyond the cutoff frequency, which is closely related to the binding strength (pulses separation).

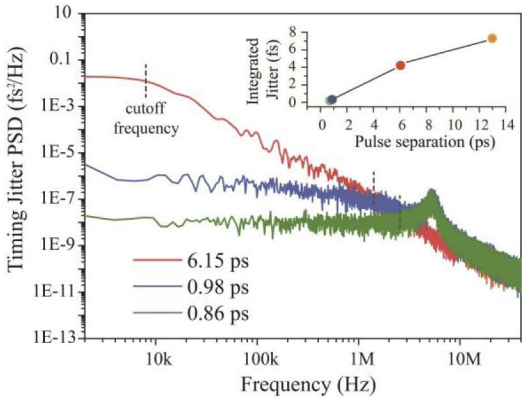

Fig. 3. Numerical simulations of intra-soliton-molecular quantum-limited timing jitter PSD. Inset: integrated quantum-limited timing jitter at corresponding pulse separation.

3. Experimental setup and Principle of OC technique

The experimental setup is schematically illustrated in Fig. 4. As shown in Fig. 4(a), a nonlinear polarization rotation (NPR) mode-locked Er-doped fiber laser is used as the platform for soliton molecules generation. A segment of 95 cm EDF with GVD about -26 ps/nm/km serves as the gain medium. The EDF is pumped through a 980/1550 nm wavelength division multiplexed (WDM) coupler. All other fibers in the cavity are standard SMF with GVD of 18 ps/nm/km. The overall optical length of the cavity is about 2.5 m, including the part of free-space bulk optics, which corresponds to 87 MHz fundamental repetition frequency. A fiber isolator is used to ensure the unidirectional transmission of pulses. The half wave plate (HWP), quarter wave plates (QWPs) and bulk polarization beam splitter (PBS) are used for NPR operation. By adjustments of pump power and waveplates, a wide range of stable single pulse operation and soliton molecules with different pulse separations can be obtained. More detailed description about high stability of the mode-locking operation can be found in [38].

Once emitted from the mode-locked fiber laser, soliton molecules are firstly directed into a Michelson-based delay line Interferometer (MI). A PBS is used to divide the laser beam into two branches. A QWP is inserted into each branch. The retro-reflected pulses are beam-combined with orthogonal polarizations and output from the other port of PBS. Temporal delay between the

Optics EXPRESS

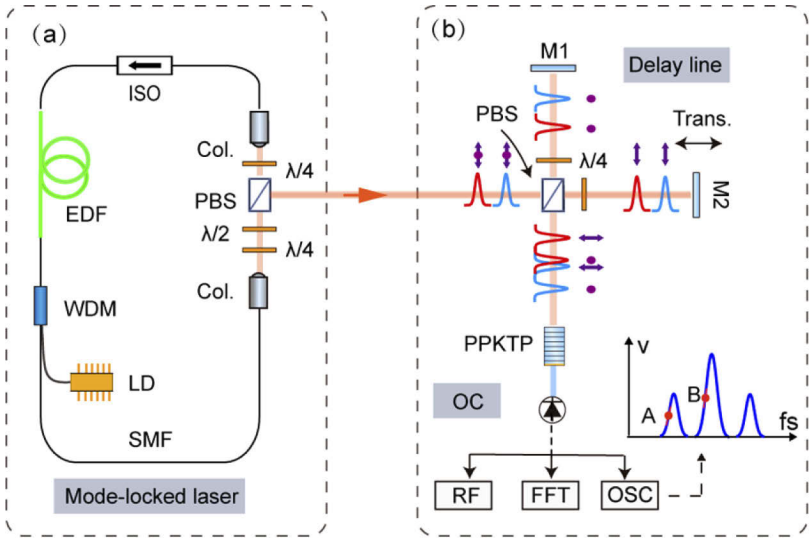

Fig. 4. (a) Experimental setup of mode-locked fiber laser. WDM, wavelength division multiplexer; ISO, isolator; Col., collimator; PBS, polarization beam splitter; λ/4, quarter wave plate; λ/2, half wave plate; (b) Principle of optical cross-correlation method; M, mirror; Trans., Translator; OC, optical cross-correlator; PPKTP, periodically poled $KTiOPO_4$. Inset, illustration of cross-correlation trace; A, Setpoint A; B, Setpoint B.

two branches is set as roughly half of the binding separation. Therefore, the rear pulse can overlap with the front pulse within the same molecule at the output of MI. Afterwards, the timing jitter of pulse separation of a soliton molecule is measured with an optical intensity cross-correlator. To this end, the combined laser beams with orthogonal polarizations are focused into a 4 mm Type-II phase-matched periodically poled $KTiOPO_4$ crystal for sum frequency generation (SFG). The inset in Fig. 4(b) shows a cross-correlation trace obtained by sweeping M2 in MI, recorded by an oscilloscope (OSC). When the leading soliton in the arm with M1 overlap with the trailing soliton in the arm with M2 exactly, the intensity of SFG signal will be proportional to the relative timing jitter, as indicated by the red point at Setpoint A, the slope of which serves as the timing error discriminator. Note that Setpoint B carries environmental noise caused by arm length perturbations of MI, instead of intrinsic intra-molecular timing jitter, since two branches of pulses are overlapped completely at Setpoint B with symmetric MI of equal arms. The SFG signals are photo-detected and recorded by an RF analyzer (RIGOL, DSA815) and an FFT analyzer (Stanford Research Systems, SR770) at high Fourier frequencies (> 100 kHz) and low Fourier frequencies (< 100 kHz), respectively. The timing jitter power spectral density can be obtained by dividing the square of timing error discriminator.

4. Experimental results and analysis

Timing jitter PSD of stationary soliton molecules are measured at Setpoint A using the optical cross-correlation method. The discriminator slope of the detected SFG signal is 1.3 mV/fs, determined by the ultrashort soliton pulse width and output power. Figure 5(a) shows the timing jitter PSD curves and integrated timing jitter at selected pulse separations. The system noise floor is shown as the gray curve, which sets the temporal resolution of the system as 1×10^{-8} fs^2/Hz. The cutoff frequency is about 10 kHz for the 6 ps pulse separation and extends to higher frequency about 50 kHz, for the smaller pulse separations of 2.23 ps. The integrated intramolecular timing jitter is 5.25 fs and 1.01 fs respectively, integrated from 100 Hz to 10 MHz Fourier frequency.

Optics EXPRESS

The corresponding optical spectrums are shown in Fig. 5(b), in which the high contrast spectral interference fringes are typical features of stationary soliton molecules.

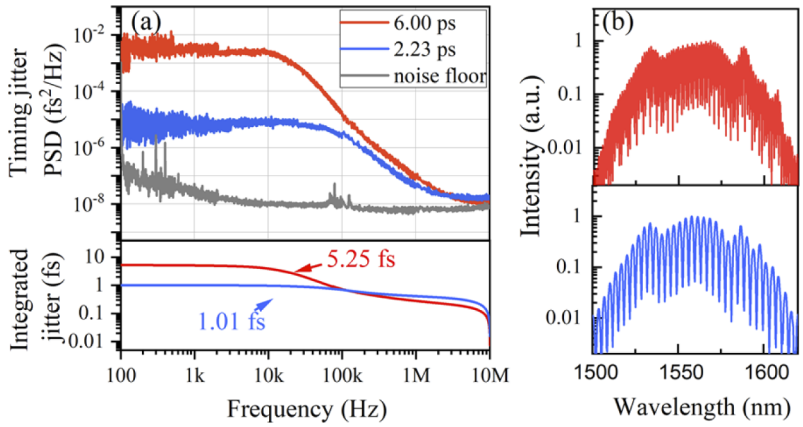

Fig. 5. (a) The upper graph, timing jitter PSD of stationary soliton molecules; The bottom graph, rms integrated timing jitter from 100 Hz to 10 MHz; (b) Optical spectrum.

To obtain a lower intra-soliton-molecular jittering, we further optimize the NCD to close-to-zero dispersion regime by cutting the fiber length of the SMF between WMD and collimator. The fiber length of this SMF has been reduced from 50 cm to 40 cm, and the NCD changed from ~-0.003 ps^2 to ~-0.0012 ps^2 accordingly. To this end, Gordon-Haus jitter indirectly coupled from ASE noise can be effectively suppressed. An ultra-narrow soliton molecule with pulse separation of 0.49 ps is experimentally obtained. As shown in the inset of Fig. 6, the corresponding modulation period of the optical spectral fringe is 16.5 nm. The intra-molecular timing jitter PSD at Setpoint A is shown by the red curve. To explore the contribution of the characterized timing jitter PSD, the noise at Setpoint B (blue curve), shot noise (green dotted line) and noise floor are also expressed. At Setpoint B, MI with equal length of arm is conducted, resulting in the noise timing jitter introduced by environmental arm length fluctuation of MI. As can be seen, the intra-molecular timing jitter PSD is limited by the noise floor at the frequency range of 100 Hz-1 kHz. For frequency range of 1-10 kHz, timing jitter PSD shows slow drifts and coherent spikes at Setpoint A, which is well aligned with the results at setpoint B. This indicates that the measurement of the intra-molecular timing jitter is dominated by environmental noise at this frequency range. Those detrimental effects located in the acoustic band (<10 kHz) could be compressed by the sound-absorbing installation or high-precision anti-vibration platform. For the frequency range above 1 MHz, shot noise from the random photon fluctuations of photodetection dominates the intra-molecular timing jitter PSD. For intermediate frequency range of 10 kHz-1 MHz, timing jitter represents the combined impression of shot noise, environmental noise and noise floor. The overall integrated timing jitter is 350 as. It is noteworthy that the quantum limited timing jitter featured of a -20 dB/decade slope is absent, which is well suppressed below the noise floor. By excluding noise contributions of the MI, which are estimated to be 260 as, a rms timing jitter < 300 as can be derived. Considering the limitation of the noise floor, the quantum-limited timing jitter of pulses separation within the soliton molecule could be further reduced. Moreover, further reduction of the intra-molecular timing jitter could be obtained by using nonlinear Fourier transform process which effectively separates the pulses from CW background or sidebands [39,40].

Optics EXPRESS

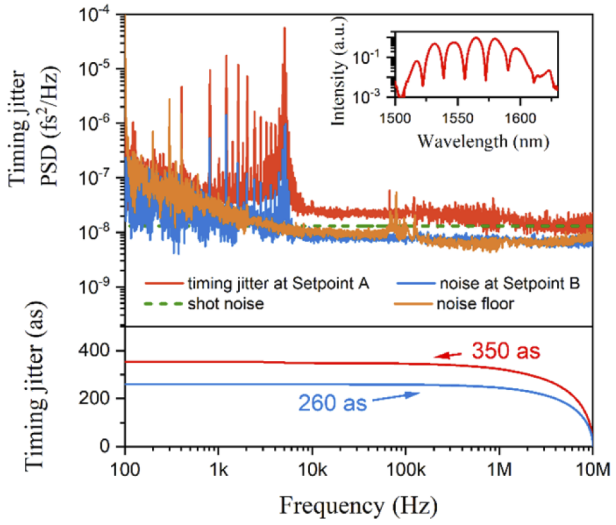

Fig. 6. (a) The upper graph, the timing jitter PSD at Setpoint A, shot noise level, noise PSD at Setpoint B and noise floor. Inset, optical spectrum; The bottom graph, rms integrated timing jitter from 100 Hz to 10 MHz at Setpoint A and Setpoint B.

5. Conclusion

In conclusion, we have investigated the timing jitter of pulse separations within soliton molecules in a mode-locked fiber laser. The intra-molecular timing jitter of soliton molecules at different separations are studied with numerical simulation and experimental measurements. In both cases, the PSD curves of intra-molecular timing jitter show low-pass characteristics with a cutoff frequency. Beyond the cutoff frequency, the PSD curves experience -20 dB/decade slope. The cutoff frequency decreases as the pulse separation increase. The comparison between simulation results and experimental measurements indicate a quantum limited intra-molecular timing jitter originated from ASE noise in the gain medium of mode-locked fiber lasers. By adjusting the NCD to close-to-zero region, the lowest intra-soliton-molecular timing jitter in a fiber laser of 350 as is obtained in experiment, with an ultra-narrow pulse separation of 0.49 ps. Despite the good agreement between experiment and simulation, it has to be pointed out that the laser mode locked by an ideal SA and gain medium in the numerical model is still simple. The slow saturable absorber effects, long range interactions such as the Casimir-like pulse interaction [41] and dynamic gain effects would be included for deeper studies in the future. We also anticipate that our results provide novel insights into soliton interacting dynamics and the understanding of related physics in complex nonlinear systems.

Funding. National Natural Science Foundation of China (Grant 61827821, Grant 61975144); State Key Laboratory of Advanced Optical Communication Systems and Networks, Shanghai Jiao Tong University (Grant 2020GZKF011).

Acknowledgments. We thank Dr. Ruoyu Liao for his kind help with numerical simulation.

Disclosures. The authors declare no conflicts of interest.

Data availability. Data underlying the results presented in this paper are not publicly available at this time but may be obtained from the authors upon reasonable request.

References

1. P. Grelu and N. Akhmediev, "Dissipative solitons for mode-locked lasers," Nat. Photonics **6**(2), 84–92 (2012).
2. M. Pang, W. He, X. Jiang, and P. S. J. Russell, "All-optical bit storage in a fibre laser by optomechanically bound states of solitons," Nat. Photonics **10**(7), 454–458 (2016).

Optics EXPRESS

3. B. A. Malomed, "Bound solitons in the nonlinear Schrödinger-Ginzburg-Landau equation," Phys. Rev. A **44**(10), 6954–6957 (1991).
4. P. Grelu, F. Belhache, F. Gutty, and J. M. Soto-Crespo, "Phase-locked soliton pairs in a stretched-pulse fiber laser," Opt. Lett. **27**(11), 966–968 (2002).
5. D. Y. Tang, W. S. Man, H.Y. Tam, and P.D. Drummond, "Observation of bound states of solitons in a passively mode-locked fiber laser," Phys. Rev. A **64**(3), 033814 (2001).
6. M. Grapinet and P. Grelu, "Vibrating soliton pairs in a mode-locked laser cavity," Opt. Lett. **31**(14), 2115–2117 (2006).
7. L. Yun and X. Liu, "Generation and propagation of bound-state pulses in a passively mode-locked figure-eight laser," IEEE Photonics J. **4**(2), 512–519 (2012).
8. K. Goda and B. Jalali, "Dispersive Fourier transformation for fast continuous single-shot measurements," Nat. Photonics **7**(2), 102–112 (2013).
9. H. J. Chen, Y. J. Tan, J. G. Long, W. C. Chen, W. Y. Hong, H. Cui, A. P. Luo, Z. C. Luo, and W. C. Xu, "Dynamical diversity of pulsating solitons in a fiber laser," Opt. Express **27**(20), 28507–28522 (2019).
10. Y. Luo, R. Xia, P. P. Shum, W. Ni, Y. Liu, H. Q. Lam, Q. Sun, X. Tang, and L. Zhao, "Real-time dynamics of soliton triplets in fiber lasers," Photonics Res. **8**(6), 884–891 (2020).
11. J. Peng, Z. Zhao, S. Boscolo, C. Finot, S. Sugavanam, D. V. Churkin, and H. Zeng, "Breather Molecular Complexes in a Passively Mode-Locked Fiber Laser," Laser Photonics Rev. **15**(7), 2000132 (2021).
12. W. He, M. Pang, DH. Yeh, J. Huang and, and P. S. J. Russell, "Synthesis and dissociation of soliton molecules in parallel optical-soliton reactors," Light Sci Appl **10**(1), 120 (2021).
13. Y. D. Cui, Y. S. Zhang, Y. J. Song, L. Huang, L. M. Tong, J. R. Qiu, and X. M. Liu, "XPM-induced vector asymmetrical soliton with spectral period doubling in mode-locked fiber laser," Laser Photonics Rev. **15**(3), 2000216 (2021).
14. A. Runge, N. Broderick, and M. Erkintalo, "Observation of soliton explosions in a passively mode-locked fiber laser," Optica **2**(1), 36–39 (2015).
15. Y. Du, Z. Xu, and X. Shu, "Spatio-spectral dynamics of the pulsating dissipative solitons in a normal-dispersion fiber laser," Opt. Lett. **43**(15), 3602–3605 (2018).
16. Z. H. Wang, Z. Zhi, Y. G. Liu, R. J. He, J. Zhao, G. D. Wang, S. C. Wang, and G. Yang, "Self-organized compound pattern and pulsation of dissipative solitons in a passively mode-locked fiber laser," Opt. Lett. **43**(3), 478–481 (2018).
17. M. Liu, Z. W. Wei, H. Li, T. J. Li, A. P. Luo, W. C. Xu, and Z. C. Luo, "Visualizing the "invisible" soliton pulsation in an ultrafast laser," Laser Photonics Rev. **14**(4), 1900317 (2020).
18. X. Liu, X. Yao, and Y. Cui, "Real-time observation of the buildup of soliton molecules," Phys. Rev. Lett. **121**(2), 023905 (2018).
19. X. Liu and Y. Cui, "Revealing the behavior of soliton buildup in a mode-locked laser," Adv. Photon. **1**, 016003 (2019).
20. G. Herink, F. Kurtz, B. Jalali, D. R. Solli, and C. Ropers, "Real-time spectral interferometry probes the internal dynamics of femtosecond soliton molecules," Science **356**(6333), 50–54 (2017).
21. K. Krupa, K. Nithyanandan, U. Andral, P. Tchofo-Dinda, and P. Grelu, "Real-Time Observation of Internal Motion within Ultrafast Dissipative Optical Soliton Molecules," Phys. Rev. Lett. **118**(24), 243901 (2017).
22. J. Peng, S. Boscolo, Z. Zhao, and H. Zeng, "Breathing dissipative solitons in mode-locked fiber lasers," Sci. Adv. **5**(11), eaax1110 (2019).
23. K. Zhao, C. Gao, X. Xiao, and C. Yang, "Real-time collision dynamics of vector solitons in a fiber laser," Photonics Res. **9**(3), 289–298 (2021).
24. H. Shi, Y. Song, C. Wang, L. Zhao, and M. Hu, "Observation of subfemtosecond fluctuations of the pulse separation in a soliton molecule," Opt. Lett. **43**(7), 1623–1626 (2018).
25. Y. Song, F. Zhou, H. Tian, and M. Hu, "Attosecond timing jitter within a temporal soliton molecule," Optica **7**(11), 1531–1534 (2020).
26. J. Kim and Y. Song, "Ultralow-noise mode-locked fiber lasers and frequency combs: Principles, status, and applications," Adv. Opt. Photonics **8**(3), 465–540 (2016).
27. H. S. Shi, Y. J. Song, T. Li, C. Y. Wang, X. Zhao, Z. Zheng, and M. L. Hu, "Timing Jitter of the Dual-Comb Mode-Locked Laser: A Quantum Origin and the Ultimate Effect on High-Speed Time- and Frequency-Domain Metrology," IEEE J. Sel. Top. Quantum Electron. **24**(5), 1–10 (2018).
28. C. Bao, M. G. Suh, B. Shen, K. Şafak, A. Dai, H. Wang, L. Wu, Z. Yuan, Q. Yang, A. B. Matsko, F. X. Kärtner, and K. J. Vahala, "Quantum diffusion of microcavity solitons," Nat. Phys. **17**(4), 462–466 (2021).
29. W. He, M. Pang, D. H. Yeh, J. Huang, C. R. Menyuk, and P. S. J. Russell, "Formation of optical supramolecular structures in a fibre laser by tailoring long-range soliton interactions," Nat. Commun. **10**(1), 5756 (2019).
30. P. Qin, S. Wang, M. Hu, and Y. Song, "Effective removal of Gordon–Haus jitter in mode-locked fiber lasers," IEEE Photonics J. **10**(1), 1–8 (2017).
31. N. Akhmediev, J. M. Soto-Crespo, and G. Town, "Pulsating solitons, chaotic solitons, period doubling, and pulse coexistence in mode-locked lasers: Complex Ginzburg-Landau equation approach," Phys. Rev. E **63**, 056602 (2001).
32. Z. Q. Wang, K. Nithyanandan, A. Coillet, P. Tchofo-Dinda, and P. Grelu, "Optical soliton molecular complexes in a passively mode-locked fibre laser," Nat. Commun. **10**(1), 830 (2019).

Optics EXPRESS

33. F. Meng, C. Lapre, C. Billet, G. Genty, and J. M. Dudley, "Instabilities and intermittence in a dissipative soliton-similariton laser using a scalar iterative map," Opt. Lett. **45**(5), 1232 (2020).
34. H. A. Haus, "Quantum noise in a solitonlike repeater system," J. Opt. Soc. Am. B **8**(5), 1122–1126 (1991).
35. H. A. Haus and A. Mecozzi, "Noise of mode-locked lasers," IEEE J. Quantum Electron. **29**(3), 983–996 (1993).
36. R. Paschotta, "Noise of mode-locked lasers (Part II): timing jitter and other fluctuations," Appl. Phys. B **79**(2), 163–173 (2004).
37. J. A. Cox, A. H. Nejadmalayeri, J. Kim, and F. X. Kärtner, "Complete characterization of quantum-limited timing jitter in passively mode-locked fiber lasers," Opt. Lett. **35**(20), 3522–3524 (2010).
38. D. Zou, Y. Zhang, Y. Song, and M Hu, "Sub-100 fs bound state solitons and period-doubling bifurcations in a mode-locked fiber laser," IEEE Photonics Technol. Lett. **32**(20), 1311–1314 (2020).
39. Y. Wang, S. Fu, C. Zhang, X. Tang, J. Kong, J. H. Lee, and L. Zhao, "Soliton distillation of pulses from a fiber laser," J. Lightwave Technol. **39**(8), 2542–2546 (2021).
40. Y. Wang, S. Fu, J. Kong, A. Komarov, M. Klimczak, R. Buczyński, X. Tang, M. Tang, Y. Qin, and L. Zhao, "Nonlinear fourier transform enabled eigenvalue spectrum investigation for fiber laser radiation," Photon. Res. **9**(8), 1531–1539 (2021).
41. K. Sulimany, O. Lib, G. Masri, A. Klein, M. Fridman, P. Grelu, O. Gat, and H. Steinberg, "Bidirectional soliton rain dynamics induced by Casimir-like interactions in a graphene mode-locked fiber laser," Phys. Rev. Lett. **121**(13), 133902 (2018).